Janus-Like 3D Tectons: Self-Assembled 2D Arrays of Functional Units at a Defined Distance from the Substrate**

David Bléger, Fabrice Mathevet, David Kreher, André-Jean Attias,* Amandine Bocheux, Sylvain Latil, Ludovic Douillard, Céline Fiorini-Debuisschert, and Fabrice Charra*

Supramolecular-based architectures onto surfaces have been widely investigated during the past two decades.[1] The most commonly employed strategies to create 2D hierarchical structures exploit noncovalent molecular interactions between planar tectons. Various approaches have been explored to generate highly ordered monocomponent structures and multicomponent assemblies.[2] In addition to the control of molecule positioning that leads to complex nanopatterns, the control of surface properties has also been addressed more recently. In that respect, nanoporous networks are of particular interest. Owing to the host properties of these networks towards organic guests, they allow for addressing various interesting aspects such as molecular dynamics, selection, recognition, and immobilization, hence leading to functional surfaces.[3]

Besides these features confined in-plane, the demanding forthcoming applications in nanotechnology require to create out-of-plane functions and to be able to fully exploit the space above the substrate. Accessing the third dimension is mandatory for the progress of for example, molecular electronics and photonics, in which the proximity of adsorbed photoactive units with conducting substrates results in a fast quenching of electronic excitations.[4] To avoid this drawback, the decoupling between active molecular units and conducting substrates is currently achieved by lifting the molecule, either by covering the surface with a uniform insulating layer[5] or through the attachment of bulky chemical side groups (e.g. *tert*-butyl groups) to the molecule, which act as spacer legs that lead to the so-called molecular "landers".[6] However, these examples suffer from limited short-range in-plane organizations. Several ways are explored to circumvent this problem based on molecular self-assembly. They consist in controlling interactions between 3D tectons, for example with H-bonded molecular "landers",[7] or in exploiting a self-assembled insulating layer as template for an upper functional layer.[8] In this context, the development of general and versatile methods for the design of 3D tectons that are able to self-assemble with long-range lateral order and to expose the desired functionality at a defined distance from the surface, remains an open challenge.

In a previous work[9] we demonstrated the 2D self-assembly of building blocks with intermolecular noncovalent bonding units (the so-called "clips") on highly-oriented pyrolytic graphite (HOPG) at the liquid–solid interface. More precisely, we showed that the attachment of clips to the lower-deck of multilayered [2.2]paracyclophane derivatives leads to the self-assembly of building blocks that are oriented face-on with the cyclophane rings that stack perpendicularly to the substrate.[10]

Herein, we introduce the concept of Janus-like 3D molecular tectons, which are doubly-functionalized building blocks that expose two opposite faces (A and B) linked by a rigid spacer. A is a pedestal designed for guiding 2D self-assembly on the substrate (HOPG) and B is a functional moiety. We show that the in-plane self-assembling ability of A controls the positioning of the out-of-plane moiety B.

As a first example to illustrate this concept, we designed and synthesized the 3D tecton **1** (Figure 1), which was obtained as a racemic mixture (**1,1′**) because of the planar chirality inherent to asymmetrically functionalized paracyclophanes.[11] The target compounds (**1,1′**) combine 1) a pedestal that consists of two molecular clips able to self-assemble on HOPG, 2) a [3.3]dithiaparacyclophane unit[12] 3.3 Å in height that acts as a two-story linker, and 3) a functional molecule, namely a distyrylbenzene fluorophore (highlighted in blue in Figure 1). This building block is designed to act as a Janus tecton, that is, it self-assembles in a well-organized in-plane monolayer and distributes the functional units according to a periodic pattern that parallels its subjacent counterpart several Å higher, thanks to the paracyclophane pillar. To confirm this behavior, STM experiments were carried out in situ, that is, at the solid–liquid interface. As a guide to the interpretation of STM images, DFT modeling has been performed on this system.

The overall synthetic route to the Janus-like building block (**1,1′**) is outlined in Scheme 1 (see the Supporting

[*] Dr. D. Bléger, Dr. F. Mathevet, Dr. D. Kreher, Prof. A.-J. Attias,
A. Bocheux
Laboratoire de Chimie des Polymères-UMR 7610
Université Pierre et Marie Curie
4 place Jussieu—case 185, 75252, Paris Cedex 05 (France)
E-mail: andre-jean.attias@upmc.fr

Dr. D. Bléger
Current address: Laboratory of Organic Chemistry and Functional
Materials, Department of Chemistry
Humboldt Universität zu Berlin
Brook-Taylor-Strasse 2, 12489 Berlin (Germany)

A. Bocheux, Dr. S. Latil, Dr. L. Douillard, Dr. C. Fiorini-Debuisschert,
Dr. F. Charra
Laboratory for Organic Electronics and Nanophotonics
Service de Physique et Chimie des Surfaces et Interfaces, IRAMIS
CEA 91191 Cedex (France)
E-mail: fabrice.charra@cea.fr

Supporting information for this article is available on the WWW under http://dx.doi.org/10.1002/anie.201008212.
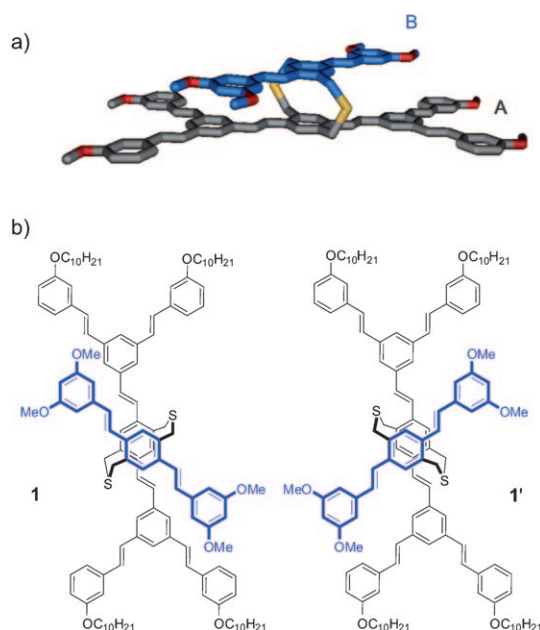
Figure 1. Janus 3D tecton. a) Structure of the two-faced building block lying on the substrate (alkyl chains are omitted for clarity), and b) chemical structures of enantiomers **1** and **1′**. The distyrylbenzene upper level (B) is highlighted in blue.

Information for experimental details). The [3.3]dithiaparacyclophane derivative **4** was assembled by condensation between the lower- and upper-deck precursors **2** and **3**. On one hand, the upper-deck of pillar **4** was functionalized by two bromo atoms suitable for subsequent Suzuki coupling with the commercial boronic ester **5**. On the other hand, the lower deck was functionalized by methylester groups which, after
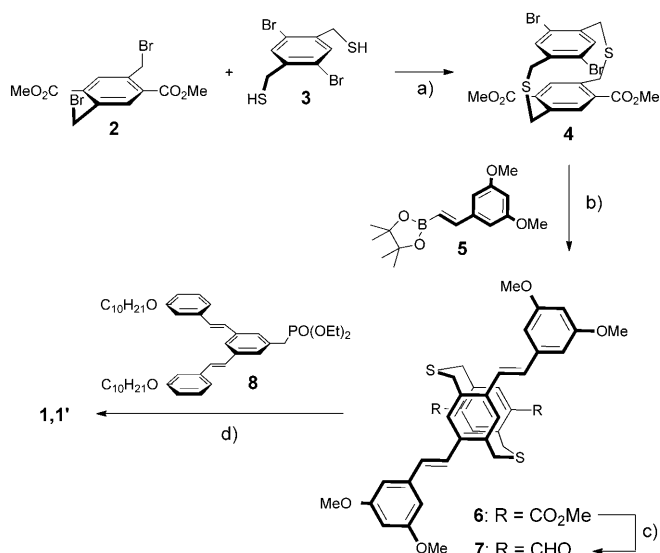
Scheme 1. Synthesis of **1**, **1′**. Reagents and conditions: a) KOH, MeOH, CH$_2$Cl$_2$, RT, 5 h; b) *trans*-2-(3,5-dimethoxyphenyl)vinylboronic acid pinacol ester **5**, [Pd(PPh$_3$)$_4$] (0.05 equiv), toluene/EtOH/H$_2$O 2:1:2, Na$_2$CO$_3$, 77°C, 5 h; c) DIBAL-H, THF, 0°C to RT, 2 h, then PCC, CH$_2$Cl$_2$, RT, 2 h; d) **8**, *t*BuOK, THF, 0°C, 1 h. DIBAL-H = diisobutylaluminum hydride, PCC = pyridinium chlorochromate.

reduction to aldehydes, were allowed to react with the phosphonate derivative **8** by a Horner–Wadsworth–Emmons reaction. The racemate (**1,1′**) was used as such for the STM experiments, that is, the two enantiomers were not separated. Remarkably, this modular synthetic approach allows for asymmetric substitution of the upper and lower decks, hence giving rise to distinct faces A and B, and is therefore highly versatile.

Figure 2 shows a short-scale STM image of the self-assembly of (**1,1′**) on a HOPG surface at the interface with an approximately 10^{-4} M solution in phenyloctane. One distinctly
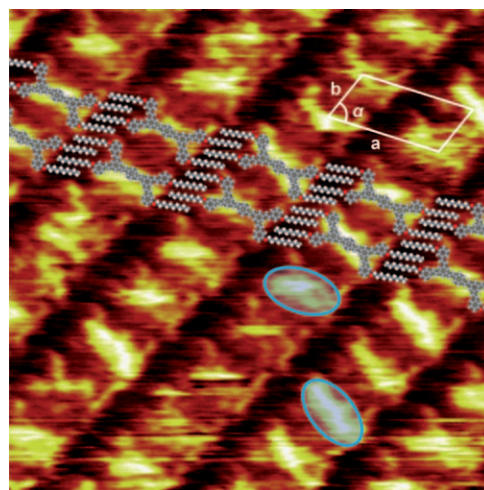

Figure 2. STM image of the self-assembly of (**1,1′**) at the HOPG–phenyloctane interface; parameters $a = 1.95 \pm 0.1$ nm, $b = 3.95 \pm 0.2$ nm, and $\alpha = 113 \pm 2°$; $V_{bias} = -1.38$ V and $I_t = 5.1$ pA (8.1×8.1 nm^2). Two distinct orientations of the ellipsoid protrusions are highlighted with blue ellipses. The scaled model of the molecular assembly of the lower level A is superimposed on the STM image (gray: carbon; red: oxygen; white: hydrogen). Distyrylbenzene upper levels B are omitted for clarity.

observes the two levels of the Janus-like compound. The bright four-armed patterns are characteristic of the lower level (face A),[9,10] and can be attributed to their rigid conjugated cores. These bright patterns alternate with darker regions that correspond either to the alkyl chains adsorbed in the Groszek geometry[13] or to uncovered parts of the HOPG (neglecting the presence of the solvent). These four-armed patterns are partially masked with brighter ellipsoids. Such features are not visible with planar building blocks that consist of face A exclusively,[14] and are thus to be attributed to the distyrylbenzene upper level (face B). The experimental lattice parameters (see Figure 2) are consistent with our previous studies.[10] Therefore, the self-assembled structures correspond to clipped molecules that form supramolecular chains (see model superimposed in Figure 2; only the pedestal, that is, face A, is drawn, distyrylbenzene upper levels B are omitted for clarity). Notice that this reconstruction breaks the axial symmetry of the graphite surface, so that two mirror-symmetric domain orientations exist, denoted R and L. In the following, only R domains are shown, R being defined as the orientation depicted in Figures 2 and 3 (see

Figure S1 in the Supporting Information for the molecules in their L conformations).

A closer inspection of the ellipsoid protrusions (faces B) reveals two distinct orientations of the longitudinal axis of the ellipses (highlighted in blue in Figure 2) relative to the lattice axes. Figure 3a shows an extended domain imaged at an increased voltage and set-point current. With such acquisition parameters, the lower level (A) is not visible anymore, each molecule appears as a bright ellipsoid protrusion only. Clearly, when discarding a few molecules that appear darker, only two distinct orientations are observable inside this specific domain. The proposed model of the self-assembly is superimposed in Figure 3a. Figure 3b shows an enlarged section, in which the two CPK models of the enantiomers are superimposed on the different ellipsoid protrusions. The two orientations of the distyrylbenzene upper levels B (in blue on the CPK model) that correspond to **1** and **1′** fit quite well with
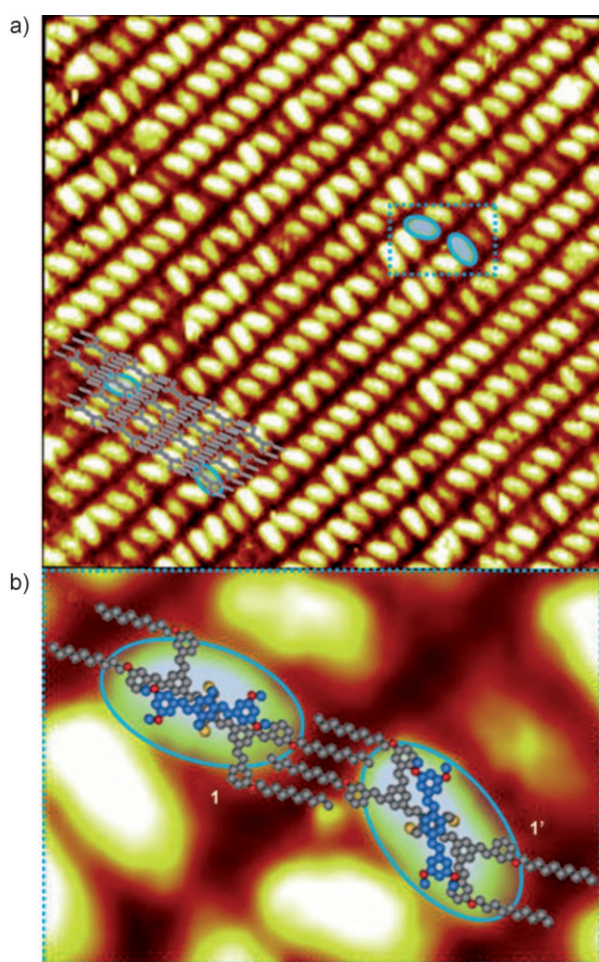

Figure 3. Insight into the self-assembly of enantiomers **1** and **1′** at the HOPG–phenyloctane interface. a) Large-scale STM image; the scaled model of the molecular assembly is superimposed on the STM picture (only lower levels A are represented for clarity); the two distinct orientations of the ellipsoids, relative to the two enantiomers **1** and **1′**, are highlighted in blue. $V_{bias} = -1.56$ V and $I_t = 27.0$ pA (49.3 × 49.3 nm²). b) Enlargement of an area of STM image 3a (delimited by the blue dashed frame) together with the model of the molecular self-assembly of **1** and **1′** (gray: lower level; blue: upper level; red: oxygen; yellow: sulfur).

the two distinct orientations of the bright ellipsoid protrusions on the STM image. These two orientations are thus the signature of the co-adsorption of **1** and **1′** in each single domain. Quantitatively, in a domain with orientation R, enantiomers are distributed according to the ratio $75 \pm 3\%$ of **1** versus $25 \pm 3\%$ of **1′** (in conformations denoted **R1** and **R1′** respectively, see Figure S1). By symmetry, the ratio is reversed for L-oriented domains, **R1** and **R1′** becoming **L1′** (mirror image of **R1**) and **L1** (mirror image of **R1′**).

Of particular interest is the process that leads to the formation of enantiomerically enriched domains. Although each species integrates a domain of its own orientation (R or L), the resulting domains are heterochiral (with the observed 3:1 ratio in favor of **1**). This interesting aspect is a direct consequence of the structure of the two-layered molecule. Indeed, the lateral organization is dictated by face A alone, whereas the chirality arises from face B. The formation of 2D heterochiral domains were already reported for chiral[15] as well as prochiral[16] molecules, even though homochiral domains are more commonly observed.

In order to gain insight into the observed distribution of **1** and **1′** according to a 3:1 ratio, full structural optimization of the 3D tectons adsorbed onto graphite (0001) was performed.[17] The optimized geometries of the two enantiomers adsorbed in an R-oriented domain are represented in Figure 4. The side views of the two enantiomers highlight the significant distortion of the upper level of **1′** compared to **1**, hence indicating a higher steric hindrance in the **1′** conformation when adsorbed in an R-oriented domain. The optimization also indicates that the **R1** configuration is more favorable than the **R1′** one (accordingly **L1′** is more favorable than **L1**), with a difference in adsorption energies as large as $\Delta E = 298$ meV (i.e. 6.9 kcal mol⁻¹).

As expected from the observed 3:1 ratio between **1** and **1′**, the energy difference ΔE is in favor of **1**. However, ΔE is about one order of magnitude higher than kT, and therefore indicates that the observed 3:1 ratio between enantiomers in a single domain cannot result from a thermodynamic equilibrium but rather from a kinetic trap. Indeed, owing to the large energy difference between configurations, it is unlikely that the differentiation occurs concomitantly with adsorption from the solution. Therefore, two R-like or L-like conformations should already be differentiated in the solution. That is, each enantiomer exists as a mixture of two conformers in the supernatant solution (see Figure S1). The presence of such conformers, which arises from hindered rotations about the two clip–cyclophane single bonds in face A, has been reported before for similar structures.[18]

If we admit the existence of two R-like (**R1**, **R1′**) and two L-like (**L1**, **L1′**) conformations of each enantiomer **1** and **1′** in solution, the most probable scenario is the following: the four species can adsorb on the surface through their face A, each isomer integrating a domain of its own orientation (R or L). Once adsorbed, the replacement of a **R1′** molecule by a more favorable **R1** ($\Delta E = 298$ meV in favor of **R1**), and respectively the replacement of **L1** by **L1′**, would require a desorption–adsorption process. However, the desorption energy of one molecule is about 4.8 eV for **R1**, as evaluated by our DFT calculations.[19] Such a high barrier prevents any desorption at
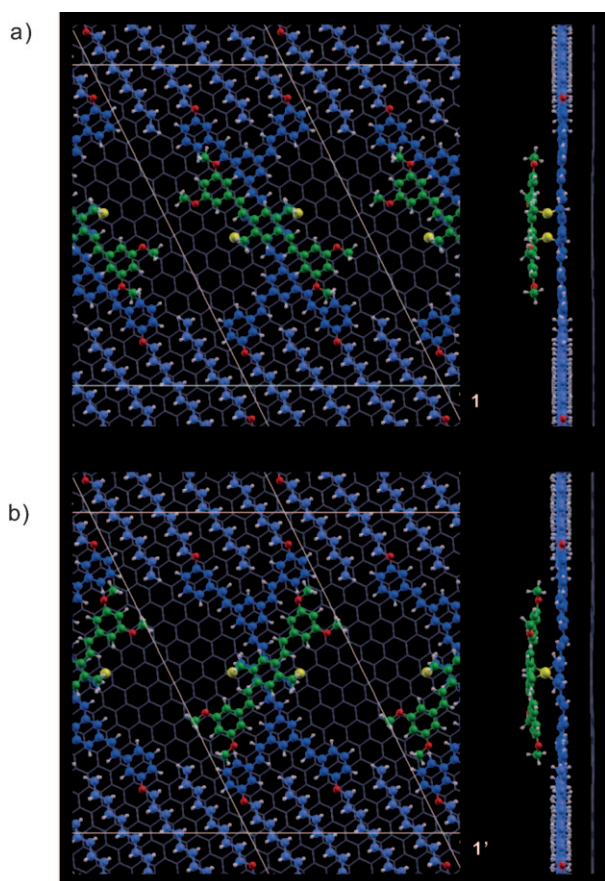
Figure 4. Representations of the epitaxial network of a) **1** and b) **1′** on HOPG, when adsorbed in an R-oriented domain, as studied by ab initio calculations (gray: HOPG surface; blue: lower level; green: upper level; red: oxygen; yellow: sulfur; white: hydrogen). In each case, a side view is displayed on the panels to the right, including the molecules (balls and sticks), and HOPG top layer (sticks only). The molecular network primitive cell is drawn in white.

estimated for molecular landers, 3.5–4.5 Å, which already permits a decoupling between molecular orbitals and the substrate, sufficient to obtain the behavior of an electronic nanowire.[21] Our estimated value is also larger than the alumina insulating layer, approximately 5 Å, which ensures a suppression of Dexter electron-exchange quenching and thus allows the luminescence of an excited fluorescent dye immobilized over a metal substrate.[5b] In our case, the optical gap of the fluorescent dye moiety is similar to that of the pedestal, and their respective HOMO and LUMO orbital levels are nearly aligned. Because of the resultant resonant coupling, the pedestal does not play the role of an insulating layer, which prevents the confinement of such an excited state. However, the versatility of our synthetic strategy makes the replacement of the current face B by a smaller bandgap chromophore possible; the excited state should thus be confined to the upper level. Ongoing research in our laboratories is concerned with this aspect.

In conclusion, the concept of doubly-functionalized 3D building blocks, the so-called Janus tectons, describes an original bottom-up route for the positioning of functional units above a conducting substrate, herein exemplified with distyrylbenzene chromophores. As shown by STM studies, the 2D self-assembled pattern of face A on the surface controls the organization of the superjacent chromophores (face B), hence leading to a periodic array of functional units at a defined distance from the substrate. The highly versatile synthetic approach presented here allows, through modification of face B, for the preparation of a wide range of 3D Janus tectons that expose various functional units ranging from fluorophores and photoswitches to molecular receptors and noncovalent binding motifs for out-of-plane host–guest systems. More generally, the bottom-up manufacturing of periodic arrays of 3D functional entities opens new perspectives towards active surfaces and interfaces.

room temperature, and instead of beeing engaged in a thermodynamic equilibrium that can usually take place at the solid–liquid interface,[20] the molecules are kinetically trapped on the surface. This result was confirmed during the STM experiments, in which no changes in the self-assembly could be detected over time (that is, all ellipsoids kept their initial orientation). Finally, since one cannot expect significant differences in the rate of adsorption of the different species, the 3:1 ratio between **R1** and **R1′** (or between their respective mirror images **L1′** and **L1**) reflects the proportion already present in solution as was obtained from synthesis.

Besides the 2D self-assembly properties, it is also possible to determine the vertical position of the face B, one of the key parameters in view of potential decoupling. As observed by STM, the apparent height of the chromophore relative to uncovered HOPG area is approximately 4.5 Å (in the conditions of Figure 2). However, because of the low conductivity of the molecules, this value is only a lower limit of the actual height. The molecular simulation reported in Figure 4 indicates a larger height difference of approximately 7 Å. Consequently, our results indicate that the vertical position of the functional unit is larger than the one

Experimental Section

STM images were acquired at room temperature with a homemade digital system. The fast scan axis was kept perpendicular to the sample slope. Images acquired simultaneously in both fast scan directions are systematically recorded and compared. All images are corrected for the drift of the instrument by combining two successive images with downward and upward slow-scan directions. The solvent was phenyloctane (Aldrich, 98%), which avoids the coadsorption often observed with linear alkanes. The substrate was HOPG (Goodfellow) and the tips were mechanically formed from a 250 mm Pt–Ir wire (Pt80/Ir20, Goodfellow). The monolayers were formed by immersing the STM junction in a droplet (ca. 10 μL) of solution immediately after cleaving the substrate and approaching the STM tip. The concentrations of the solutions were around 10^{-4}M and the solutions were systematically heated prior to deposition on the HOPG surface.

Full structural optimization of the complete paracyclophane molecules adsorbed onto graphite (0001) were performed using ab initio calculations. The graphite surface was approximated by a single layer; further details are given in the Supporting Information.

[1] a) S. De Feyter, F. C. De Schryver, *Chem. Soc. Rev.* **2003**, *32*, 139–150; b) J. V. Barth, G. Costantini, K. Kern, *Nature* **2005**, *437*, 671–679; c) J. V. Barth, *Annu. Rev. Phys. Chem.* **2007**, *58*, 375–407; d) A. Ciesielski, C. A. Palma, M. Bonini, P. Samorì, *Adv. Mater.* **2010**, *22*, 3506–3520; e) L. Bartels, *Nat. Chem.* **2010**, *2*, 87–95.

[2] a) K. W. Hipps, L. Scudiero, D. E. Barlow, M. P. Cooke, *J. Am. Chem. Soc.* **2002**, *124*, 2126–2127; b) L. Scudiero, K. W. Hipps, D. E. Barlow, *J. Phys. Chem. B* **2003**, *107*, 2903–2909; c) J. A. Elemans, S. Lei, S. De Feyter, *Angew. Chem.* **2009**, *121*, 7434–7469; *Angew. Chem. Int. Ed.* **2009**, *48*, 7298–7332; d) Y. Yang, C. Wang, *Chem. Soc. Rev.* **2009**, *38*, 2576–2589.

[3] a) F. Cicoira, C. Santano, F. Rosei, *Top. Curr. Chem.* **2008**, *285*, 203–267; b) D. Bonifazi, S. Mohnani, A. Llanes-Pallas, *Chem. Eur. J.* **2009**, *15*, 7004–7025, and references therein; c) T. Kudernac, D. Lei, J. A. A. W. Elemans, S. De Feyter, *Chem. Soc. Rev.* **2009**, *38*, 402–421; d) S. Furukawa, S. De Feyter, *Top. Curr. Chem.* **2009**, *287*, 87–133.

[4] a) D. L. Mills, J. X. Cao, R. Wu, *Phys. Rev. B* **2007**, *75*, 205439; b) J. Repp, G. Meyer, S. M. Stojkovic, A. Gourdon, C. Joachim, *Phys. Rev. Lett.* **2005**, *94*, 026803.

[5] a) H. Rauscher, T. A. Jung, J. L. Lin, A. Kirakosian, F. J. Himpsel, U. Rohr, K. Müllen, *Chem. Phys. Lett.* **1999**, *303*, 363–367; b) X. H. Qiu, G. V. Nazin, W. Ho, *Science* **2003**, *299*, 542–546.

[6] a) R. Otero, Y. Naitoh, F. Rosei, P. Jiang, P. Thostrup, A. Gourdon, E. Laegsgaard, I. Stensgaard, C. Joachim, F. Besenbacher, *Angew. Chem.* **2004**, *116*, 2144–2147; *Angew. Chem. Int. Ed.* **2004**, *43*, 2092–2095; b) M. Alemani, M. V. Peters, S. Hecht, K. H. Rieder, F. Moresco, L. Grill, *J. Am. Chem. Soc.* **2006**, *128*, 14446–14447; c) M. J. Comstock, N. Levy, A. Kirakosian, J. Cho, F. Lauterwasser, J. H. Harvey, D. A. Strubbe, J. M. Frechet, D. Trauner, S. G. Louie, M. F. Crommie, *Phys. Rev. Lett.* **2007**, *99*, 038301; d) C. Dri, M. V. Peters, J. Schwarz, S. Hecht, L. Grill, *Nat. Nanotechnol.* **2008**, *3*, 649–653.

[7] M. Yu, N. Kalashnyk, W. Xu, R. Barattin, Y. Benjalal, E. Laegsgaard, I. Stensgaard, M. Hliwa, X. Bouju, A. Gourdon, C. Joachim, F. Besenbacher, T. R. Linderoth, *ACS Nano* **2010**, *4*, 4097–4109.

[8] D. den Boer, T. Habets, M. J. J. Coenen, M. van der Maas, T. P. J. Peters, M. J. Crossley, T. Khoury, A. E. Rowan, R. J. M. Nolte, S. Speller, J. A. A. W. Elemans, *Langmuir* **2011**, *27*, 2644–2651.

[9] D. Bléger, D. Kreher, F. Mathevet, A. J. Attias, G. Schull, A. Huard, L. Douillard, C. Fiorini-Debuischert, F. Charra, *Angew. Chem.* **2007**, *119*, 7548–7551; *Angew. Chem. Int. Ed.* **2007**, *46*, 7404–7407.

[10] D. Bléger, D. Kreher, F. Mathevet, A. J. Attias, I. Arfaoui, G. Metge, L. Douillard, C. Fiorini-Debuisschert, F. Charra, *Angew. Chem.* **2008**, *120*, 8540–8543; *Angew. Chem. Int. Ed.* **2008**, *47*, 8412–8415.

[11] a) *Modern Cyclophane Chemistry* (Eds.: R. Gleiter, H. Hopf), Wiley-VCH, Weinheim, **2004**; b) A. Muranaka, M. Shibahara, M. Watanabe, T. Matsumoto, T. Shinmyozu, N. Kobayashi, *J. Org. Chem.* **2008**, *73*, 9125–9128.

[12] See W. L. Wang, J. W. Xu, Y. H. Lai, *Org. Lett.* **2003**, *5*, 2765–2768 for the X-ray structure of [3.3]dithiaparacyclophanes.

[13] A. J. Groszek, *Proc. R. Soc. London Ser. A* **1970**, *314*, 473.

[14] See Figure 1 (compound **I**) in reference [10].

[15] See for example a) S. De Feyter, A. Gesquiere, K. Wurst, D. B. Amabilino, J. Veciana, F. C. De Schryver, *Angew. Chem.* **2001**, *113*, 3317–3320; *Angew. Chem. Int. Ed.* **2001**, *40*, 3217–3220; b) R. Fasel, M. Parschau, K. H. Ernst, *Nature* **2006**, *439*, 449–452; c) S. Haq, N. Liu, V. Humblot, A. P. J. Jansen, R. Raval, *Nat. Chem.* **2009**, *1*, 409–414.

[16] F. Vidal, E. Delvigne, S. Stepanow, N. Lin, J. V. Barth, K. Kern, *J. Am. Chem. Soc.* **2005**, *127*, 10101–10106.

[17] See Supporting Information for the DFT modeling details.

[18] It has been observed in similarly-substituted cyclophanes that even less bulky substituents hinder the rotation about the substituent-cyclophane single bond, thus leading to the existence of two conformers in the solution: see W. L. Wang, J. Xu, Z. Sun, X. Zhang, Y. Lu, Y. H. Lai, *Macromolecules* **2006**, *39*, 7277–7285.

[19] Neglecting the two dimensional crystallization energy associated with the close packing of the aliphatic chains.

[20] S. B. Lei, K. Tahara, F. C. De Schryver, M. Van der Auweraer, Y. Tobe, S. De Feyter, *Angew. Chem.* **2008**, *120*, 3006–3010; *Angew. Chem. Int. Ed.* **2008**, *47*, 2964–2968.

[21] F. Moresco, L. Gross, M. Alemani, K. H. Rieder, H. Tang, A. Gourdon, C. Joachim, *Phys. Rev. Lett.* **2003**, *91*, 036601.